



J. Serb. Chem. Soc. 87 (6) 693–706 (2022)
JSCS–5551

***In silico* identification of novel allosteric inhibitors of Dengue virus NS2B/NS3 serine protease**

RENATO A. DA COSTA¹, JOÃO A. P. DA ROCHA^{2*}, ALAN S. PINHEIRO³,
ANDRÉIA S. S. DA COSTA⁴, ELAINE C. M. DA ROCHA⁵, LUIZ P. C. JOSINO³,
ARLAN DA SILVA GONÇALVES⁶, ANDERSON H. L. LIMA³ and DAVI S. B. BRASIL⁴

¹Federal Institute of Education, Science and Technology of Pará - Campus Castanhal, 68740-970, Castanhal-PA, Brazil, ²Federal Institute of Education, Science and Technology of Pará - Campus Bragança, 68600-000, Bragança-PA, Brazil, ³Graduate Program in Chemistry, Institute of Exact and Natural Sciences, Federal University of Pará (UFPA), 66075-110 Belém-PA, Brazil, ⁴Graduate Program in Science and Environment, Institute of Exact and Natural Sciences, Federal University of Pará (UFPA), 66075-110 Belém-PA, Brazil, ⁵Federal Rural University of the Amazon Campus Capanema (UFRA), 68700-665 Capanema-PA, Brazil and ⁶Federal Institute of Education, Science and Technology of Espírito Santo Campus Vila Velha, 29106-010 Vila Velha-ES, Brazil

(Received 29 September 2021, revised 20 January, accepted 17 February 2022)

Abstract: Although dengue is a disease that affects more than 100 countries and puts almost 400 million lives at risk each year, there is no approved antiviral in the treatment of this pathology. In this context, proteases are potential biological targets since they are essential in the replication process of this virus. In this study, a library of more than 3,000 structures was used to explore the allosteric inhibition of the NS2B/NS3 protease complex using consensual docking techniques. The results show four best ranked structures that were selected for molecular dynamics and free energy simulations. The present analysis corroborates with other studies (experimental and theoretical) presented in the literature. Thus, the computational approach used here proved to be useful for planning new inhibitors in the combat against Dengue disease.

Keywords: NS2B/NS3pro; consensual docking; molecular dynamics; binding free energy calculations.

INTRODUCTION

Dengue is a disease caused by the dengue virus (DENV), which affects the tropics and subtropics and is transmitted by the *Aedes aegypti*. In more than 100 countries, the virus causes approximately 390 million infections per year. DENV infections can result in several clinical conditions, even leading to death.^{1–3} Not-

* Corresponding author. E-mail: joao.rocha@ifpa.edu.br
<https://doi.org/10.2298/JSC210929011D>

ably, there are no approved antiviral drugs for this disease and, currently, patients are treated with supportive care to relieve fever, pain, and dehydration.⁴ Therefore, a new strategy is needed to discover potential antiviral agents for treating the dengue virus. The success of such research lies in finding protease enzymes that are indispensable for virus replication and for maintaining its infectivity. For this purpose, the NS2B/NS3 protease (NS2B/NS3pro) complex appears promising, as it is necessary for processing at the junctions of NS2A/NS2B, NS2B/NS3, NS3/NS4A and NS4B/NS5, NS3, NS2A and NS4A in dengue, and is therefore an important target for the development of drugs against dengue infection.^{5,6} Most studies targeting NS2B-NS3pro by small-molecule inhibitors have focused on the active site, but unfortunately none of the drugs that inhibit the enzyme by binding to the active site have been approved to date. The flat and charged nature of the NS2B-NS3pro active site may be responsible for the difficulties in the development of inhibitors, which suggests that a strategy for exploring allosteric sites may be useful.⁷

A promising strategy is to design small molecules directed at the allosteric site.⁸ Allosteric sites are defined as regions of a protein that, when linked to a small ligand, change the conformation or change the conformational balance, affecting the enzyme function. Allosteric sites have previously been considered important in proteases, making the exploration of allosteric sites in DENV NS2B-NS3pro promising.⁹ Thus, in this work, the results of virtual screening (VS), consensual docking, molecular dynamics (MD), and free energy calculations for a bank of molecules that may be active against the DENV NS2B/NS3pro allosteric site are presented. This study is expected to contribute to the discovery of novel and potent anti-dengue agents. The use of molecular-scale methods for the discovery of new potential active ligands, as well as binding sites for unknown target proteins, is now an established reality. The literature offers many success stories of active compounds developed from insights obtained *in silico* and approved by the Food and Drug Administration (FDA). One of the most famous examples is raltegravir, an inhibitor of HIV integrase, developed after the discovery of a transient binding area through molecular dynamics simulations. These simulations in biomolecules and biomacromolecules are an interesting and fast method that is increasingly contributing to the fundamental understanding of living organisms, as well as having a profound impact on numerous diverse scientific endeavors, from biotechnological applications such as the manufacture of new intelligent biomaterials, DNA sequencing and the treatment of disease and drug development. Using computer modeling to complement experiments is helping to bridge the gap between atomic-level properties with whole-organism function, an effort that cannot be accomplished by either approach in isolation. A combination of several computational techniques, span-

ning a wide range of time and size scales, is ideal for capturing information at biological scales.^{10,11}

EXPERIMENTAL

Virtual screenings and consensual docking

A library of 3940 compounds from the BaSe FilTer¹² (Part 1/20 of the total compounds present in the bank) were submitted to a VS and subsequently to a consensus analysis. The crystallographic coordinates of the DENV NS2B/NS3pro enzyme (PDB code: 2FOM)¹³ retrieved from the Protein Data Bank (PDB) were used as a model of the biological target.

Consensual docking is an approach that consists of combining the results obtained by different scoring functions and ranking them, according to the combination of the results, improving the results obtained and compensating for the deficiencies found in each scoring function.¹⁴ Thus, consensus analysis is considered more efficient than single scoring for molecular docking and represents an effective way to achieve better hit rates in various VS studies.^{15,16} In both programs, fluctuations of the enzyme and the ligands were not allowed. Therefore, the docking results were analyzed using different protocols to obtain the most consistent binding affinity of the ligands. First, a VS was performed with the compounds in DENV NS2B/NS3pro using two programs: CSDGOLD¹⁷ and DOCK6.¹⁸ The CSDGOLD program uses the empirical fitness function called ChemPLP, which consists of applying hydrogen and metal bonding terms and piecewise linear potential (PLP) to model the steric complementarity between the protein and the ligand. The dimensionless scoring scale measures the success of the pose; higher scores indicate better docking positions.¹⁷ The DOCK6 program is characterized by the use of an incremental construction algorithm. The scoring functions that guide the ligands to the target are based on a grid of potential energy, where van der Waals interactions are assessed by Lennard–Jones potentials, and the electrostatic interactions are evaluated through time-dependent dielectric functions.¹⁸

To perform molecular docking calculations, the coordinates for the search box were positioned based on the position of the allosteric binding site DENV NS2B/NS3pro according to.¹⁹ For the CSD-GOLD protocol, the following parameters were set for the ChemPLP algorithm: all water molecules and ions were removed, then the coordinates for the search box were centered in $x = -10.004$, $y = -8.839$ and $z = 7.879$. For the DOCK6 protocol, the hydrogens were removed from the crystallographic model, and a box of 10 Å in size was generated and calculated by the dms, SPHGEN, grid and SHOWBOX programs.^{20,21}

The consensual docking analysis was performed using the scaled-rank-by-number method. The scaled-rank-by-number is employed by scoring the energy values predicted for all compounds in the molecular docking with the different programs, according to Eq. (1):

$$X_{\text{ranked}} = (X - X_{\text{min}})/(X_{\text{max}} - X_{\text{min}}) \quad (1)$$

where the scored value is obtained; X_{max} and X_{min} are, respectively, the maximum and minimum values of the utilized set. X_{max} corresponds to the most favorable affinity energy (lowest energy value), *i.e.*, X_{ranked} equals 1; the least favorable affinity energy value (highest energy value) is assigned 0, *i.e.*, X_{ranked} equals 0. The respective values scored for the compounds are then summed up in each program, and the final rank of the compounds that were best scored by different scoring functions is obtained.²²

Molecular dynamics simulations

For analyze conformational changes in proteins and ligand structures, as well as the stability of ligand-receptor complexes, MD simulations were performed using the Amber18 pack-

age. Amber ff14SB and the amber general force field (GAFF) were applied to treat the structures of the protein and the four ligands best scored by the consensual dock, respectively.^{23,24}

The atomic charges of the ligands were calculated using the restrained electrostatic potential (RESP) protocol at the HF/6-31G* level of theory²⁵ using the Gaussian 09 software²⁶ (see Supplementary material to this paper). First, the protonation states of the ionizable residues of the protein structures were analyzed by p*K*_a calculation at neutral pH using the H⁺⁺ server.²⁷ All systems were solvated in the Leap module using a cubic water-box with the TIP3P model.²⁸ Na⁺ was added to maintain the electroneutrality of the systems. All hydrogen atoms were minimized by 2000 steps of steepest descent, followed by 3000 steps of conjugate gradient algorithm. Next, the positions of the water molecules were relaxed using the same protocol. The whole system was energy-minimized for 5000 steps of the steepest descent plus 5000 steps of conjugate gradients. Thereafter, the system was heated from 0 to 300 K running 200 ps of MD and, next, 300 ps to density equilibration with position of the starting restraints on the protein-ligand atoms at a constant volume. Before performing the production step, all protein-ligand systems were equilibrated with 500 ps of MD without positional restraints at a constant pressure. The temperature was maintained at 300 K by coupling to a Langevin thermostat using a collision frequency of 2 cm⁻¹. A cutoff of 8 Å was employed for non-bonded interactions, the particle mesh Ewald (PME)²⁹ method and the Shake³⁰ algorithm were used to restrict the bond lengths involving the hydrogen atoms. Finally, the MD simulations (production) were performed using 100 ns at a temperature of 300 K without positional restraints. The generated trajectories were used to analyze the behavior of each complex to access the stability of the system in the explicit water environment. The deviations of the protein and protein–ligand complex system was analyzed by calculating root mean square deviation (*RMSD*), root mean square fluctuation (*RMSF*), radius of gyration (*RG*) and solvent accessible surface area (*SASA*).

Generalized Born and surface area continuum solvation (MM/GBSA)

End-point methods are strategies to perform binding free energy calculations in structure-based drug discovery, known for their accuracy/time consuming advantage, once it is considered the end of trajectory simulations as sample, where theoretically it should have a more stable structure, with lower *RMSD* fluctuation values through MD simulations. Therefore, using these methods to perform predictions about the strength of a receptor–ligand type of structure is advantageous, and usually more accurate than the scoring functions implemented in molecular docking.³¹

A widely used method in the literature is the molecular mechanics/generalized-Born surface area (MM/GBSA) method that was first implemented in studies with RNA and DNA complexes.³²

The MM/GBSA method was applied to estimate the binding free energy change (ΔG_{bind}).³³ The last 10 ns of MD simulations of each system were used for binding free energy calculations.

ΔG_{bind} can be calculated according to the Eqs. (2)–(5):

$$\Delta G_{\text{bind}} = G_{\text{complex}} - (G_{\text{protein}} - G_{\text{ligand}}) \quad (2)$$

$$\Delta G_{\text{bind}} = \Delta H - T\Delta S \approx \Delta E_{\text{MM}} + \Delta G_{\text{solv}} - T\Delta S \quad (3)$$

$$\Delta E_{\text{MM}} = \Delta E_{\text{internal}} + \Delta E_{\text{electrostatic}} + \Delta H_{\text{vd}} \quad (4)$$

$$\Delta G_{\text{solv}} = \Delta G_{\text{GB}} + \Delta G_{\text{nonpol}} \quad (5)$$

where ΔG_{bind} is the inhibitor–protein binding free energy change resulting from the sum of the molecular mechanic energy (ΔE_{MM}), the desolvation free energy change (ΔG_{solv}) and the

entropic change term ($-T\Delta S$). The gas-phase molecular mechanic energy change (ΔE_{MM}) can be described by the sum of the internal energy contributions ($\Delta E_{\text{internal}}$), the sum of the energies due to the bonds, angles and dihedrals, electrostatic contributions ($\Delta E_{\text{electrostatic}}$), and the van der Waals term (ΔE_{vdw}). The desolvation free energy change (ΔG_{solv}) is the sum of the polar (ΔG_{GB}) and non-polar (ΔG_{nonpol}) contributions. The polar desolvation term was calculated using the implicit generalized Born (GB) approach. The entropic contribution explicit by the term $-T\Delta S$ in Eq. (3) is often disregarded when one is interested in relative and not absolute free energies, because it is significantly costly to compute entropic conformational changes.³¹ In this work ligands with similar structures were analyzed, and for this reason a normal mode calculation was not used for this analysis because of computational cost and the tendency to have a large margin of error, introducing compelling uncertainty to the final result.

Per-residue energy decomposition

A per-residue energy decomposition method was used to determine the total energy contribution of each residue to the drug–receptor interaction and also to investigate the chemical nature of its interactions.³⁴

MM/GBSA allows analysis of the contributions of individual residues or energetic terms by free energy decomposition analysis, which provides detailed energetic contributions to each specific amino acid residue sidechain to the binding state of the system, identifying the leading interactions in the binding process. That information can help further researchers to get a drug developed with the help of theoretical studies in the complex formation with proteins or another receptor type.

The interaction energy between an inhibitor and every residue in an enzyme could be described, according to Eq. (5), as the sum of van der Waals (ΔE_{vdw} terms) and electrostatic (ΔE_{ele}) contributions in the gas phase, and polar (ΔG_{pol}) and nonpolar solvation (ΔG_{nonpol}) contributions:

$$\Delta G_{\text{inhibitor-residue}} = \Delta E_{\text{vdw}} + \Delta G_{\text{ele}} - \Delta G_{\text{pol}} + \Delta G_{\text{nonpol}} \quad (6)$$

RESULTS AND DISCUSSION

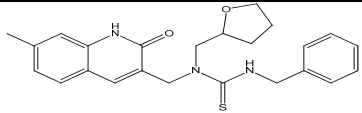
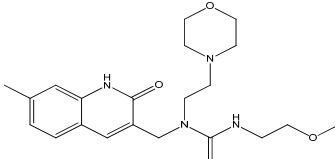
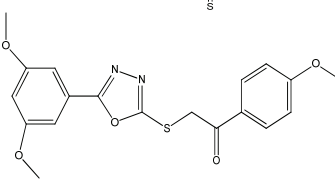
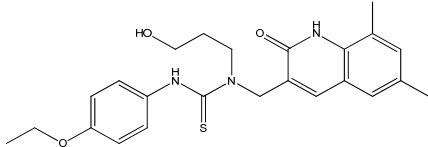
Analysis of selectivity of ligands to DENV-2 NS2B/NS3pro allosteric binding pockets

VS was performed for 3940 compounds and the efficacy of these compounds against DENV-2 NS2B/NS3pro was evaluated using consensual molecular docking, MD simulations, and binding free energy calculations. First, the docking scores obtained from GOLD and DOCK6, as well as the number of H-bond interactions formed with the amino acid residues from protein allosteric site, were analyzed. The consensual scoring values obtained for all 3940 compounds bound to the DENV-2 NS2B/NS3pro structure are given in Table S-I (Supplementary material). The results demonstrated that compounds 33-P5, 3-P5, 1466-P6 and 2645-P15 showed the best consensus docking rank. Thus, these ligands were selected for the MD simulation. The final ranks are listed in Table I.

Molecular docking is a powerful computational method used to investigate the selectivity and affinity of a ligand in a macromolecular receptor,³⁵ and has been widely applied in structure-based virtual screening approaches combined with *in silico* MD simulation techniques, and in calculating the free energy of

binding in the search for allosteric inhibitors of DENV-2 NS2B/NS3pro.³⁶⁻³⁸ Based on the consensual docking results, the four best compounds were selected for analyzing the conformational dynamics of the complexes and their binding affinities.

TABLE I. Consensual docking rank final of four compounds docked against the DENV-2 NS2B/NS3pro structures

| Compound ID | Rank final | Structure |
|-------------------|------------|--|
| Compound_33-P5 | 1.65 |  |
| Compound_3-P5 | 1.64 |  |
| Compound_2645-P15 | 1.63 |  |
| Compound_1466-P6 | 1.62 |  |

Molecular dynamics

The four best compounds were selected for MD simulation analysis to assess their stability and conformational changes, and to understand the dynamic characteristics of these ligands in relation to time in nanoseconds. Overall, the backbone *RMSD* values for Apo NS2B/NS3, NS2B/NS3pro-3-P5, NS2B/NS3pro-33-P5, NS2B/NS3pro-1466-P6 and NS2B/NS3pro-2645-P15 are $< 3 \text{ \AA}$ throughout the 100 ns simulation time, reflecting the stability of the systems. Fluctuations between 1 and 3 \AA within a reference protein structure are perfectly acceptable and indicate the stability of the complex.³⁹ Note that ligand 1466-P6 showed the highest *RMSD* value of $\approx 2.5 \text{ \AA}$, lightly greater than the *RMSD* value for the free protein (Apo). We believe that this ligand is undergoing a process of reaccommodation in the allosteric site. The 3-P5 and 2645-P15 ligands showed the lowest *RMSD* values of 1.4 and 1.7 \AA , respectively, even less than the value for free protein (Apo, Fig. 1). This fact may suggest that these two simulated ligands have high affinity for the protein.

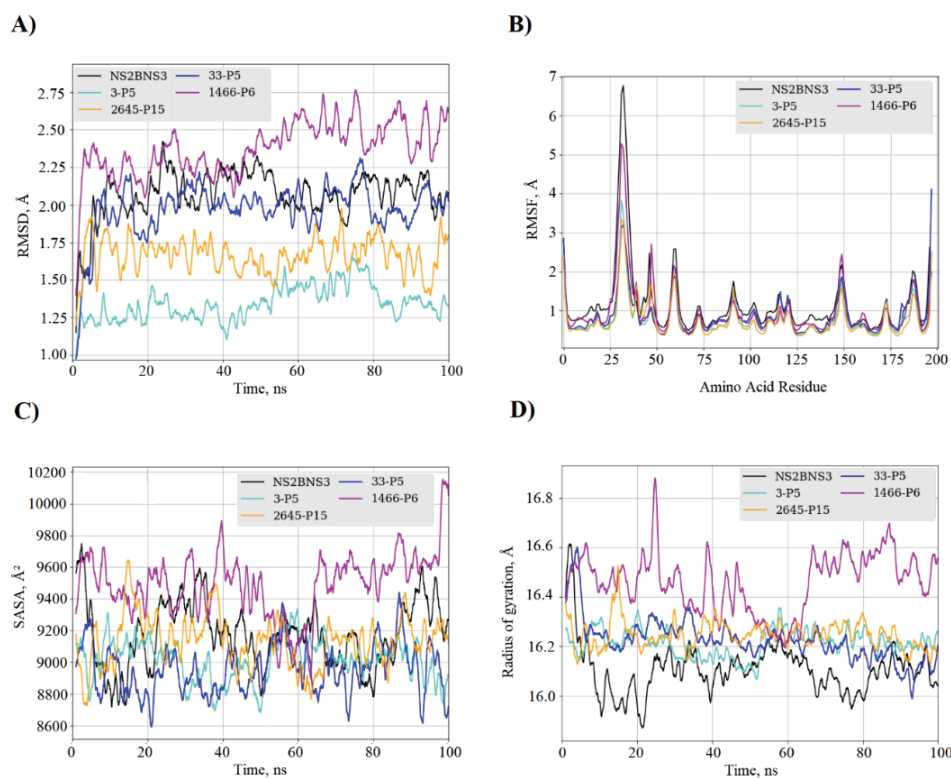


Fig. 1 Structural dynamics of NS2B/NS3pro enzyme-ligand complexes (3-P5 in cyan, 33-P5 in blue, 1466-P6 in magenta and 264-P15 inhibitor in orange) and unbounded Apo (black) during 100 ns of MD simulations. A) $C\alpha$ backbone $RMSD$ in Å of all the selected compounds bound to the NS2B/NS3pro enzyme; B) $RMSF$ values in Å plotted against the residue number for all the selected compounds bound to the NS2B/NS3pro enzyme; C) $SASA$ values of the $C\alpha$ backbone atoms; D) Rg values after compound binding.

The $RMSF$ values (Fig. 1B) support this hypothesis. The highest fluctuations correspond to free protein and the 1466-P6 ligand, while the lowest values are attributed to systems complexed with ligands 3-P5 and 2645-P15, suggesting that these systems are more stable.

A solvent accessible surface area ($SASA$) analysis was performed to define the hydrophobicity of the protein in relation to the solvent. An $SASA$ analysis is important for an energetic evaluation of biological macromolecules.⁴⁰ The $SASA$ results for all systems during 100 ns of MD simulations are shown in Fig. 1C. The average $SASA$ values for the APO protein and the complexes 3-P5-NS2B/NS3, 33-P5-NS2B/NS3, 1466-P6-NS2B/NS3 and 2645-P15-NS2B/NS3 were, respectively, 9176 (black), 9014 (cyan), 8955 (blue), 9499 (magenta) and 9132 Å² (orange), showing that the systems NS2B/NS3-ligands were relatively more stable.

A calculation of the radius of gyration (R_g) was performed to evaluate the stability of the protein–ligand systems by calculating the structural compactness along the MD trajectories.⁴¹ After the MD simulation calculation, the calculation of R_g was also used to determine the stability of the folded and unfolded protein, and the complexes system. A graph of R_g as a function of time for the protein and all the protein-ligand complexes (NS2B/NS3pro-3-P5, NS2B/NS3pro-33-P5, NS2B/NS3pro-1466-P6 and NS2B/NS3pro-2645-P15) is shown in Fig. 1D. The average R_g value of the Apo protein was 16,10 Å (black). The average R_g value of the complexes were 16.21 (cyan), 16.22 (blue), 16.46 (magenta) and 116.24 Å (orange), respectively. It was found that all complexes exhibited relatively similar and consistent R_g values as compared to the Apo protein, which indicates that these are perfectly superimposed with each other and have good stability. Since the radius of gyration had a relatively consistent value throughout the MD simulation, it was regarded as stably folded.⁴²

To further explore the binding mode of the complexes, the MMGBSA method was applied to the simulated systems, and the values of the free energies and their components for the complexes formed between DENV-2 NS2B/NS3pro ligands 3-P5, 33-P5, 1466-P6 and 2645-P15 indicated that the formation of the four complexes was favorable. The ΔG_{bind} and the values of the van der Waals energy change (ΔE_{vdW}), and the electrostatic (ΔE_{ele}), polar (ΔG_{GB}), and non-polar (ΔG_{nonpol}) contributions are summarized in Table II. Based on the binding free energy calculations, the complex of ligand 2645-P15 with DENV-2 NS2B/NS3pro showed the lowest affinity energy change (ΔG_{bind}) based on the MM/GBSA method.

TABLE II. Affinity energy values (J mol^{-1}) and energy components. ΔE_{vdw} , van der Waals contributions; ΔE_{ele} , electrostatic contributions; ΔG_{GB} , polar contributions; ΔG_{np} , non-polar contributions; ΔG_{bind} , affinity energy; the values \pm correspond to the standard error of the mean

| Ligand ID | ΔE_{vdW} | ΔE_{ele} | ΔG_{GB} | ΔG_{NP} | ΔG_{bind} |
|-----------|-------------------------|-------------------------|------------------------|------------------------|--------------------------|
| 3-P5 | -184765.44 | -70165.68 | 158531.76 | -23346.72 | -120624.72 |
| | ± 376.56 | ± 962.32 | ± 878.64 | ± 376.56 | ± 334.72 |
| 33-P5 | -136440.24 | -118323.52 | 175142.24 | -15899.20 | -95478.88 |
| | ± 418.4 | ± 962.32 | ± 920.48 | ± 41.84 | ± 376.56 |
| 1466-P6 | -174682.00 | -66818.48 | 149619.84 | -21296.56 | -113135.36 |
| | ± 460.24 | ± 794.96 | ± 711.28 | ± 41.84 | ± 418.40 |
| 2645-P15 | -199200.24 | -36066.08 | 117235.68 | -24016.16 | -140164.00 |
| | ± 292.88 | ± 627.60 | ± 543.92 | ± 251.04 | ± 334.72 |

The main energetic contributions to the interaction of the DENV-2 NS2B/NS3pro receptor with the ligands are van der Waals contributions. It was observed that the energetic contribution of the hydrophobic residues of Leu106 (76), Trp113 (83), Ile153 (123), Val184 (154), Ala194 (164) and Ala196 (166), are present in the DENV NS2B/NS3pro allosteric site;^{38,43} the numbers in paren-

theses indicate the numbering in the Erbel¹⁶ model. In general, this is the preferred type of interaction observed between the complexes under study and protein residues.⁴⁴ To a lesser extent, electrostatic and nonpolar contributions also favored system formation.

The energy contributions in the simulations of each residue to the four complexes are shown in Fig. 2. This energy decomposition analysis shows the residues that contribute most significantly to the total interaction energy and, therefore, to the stabilization of the complexes.

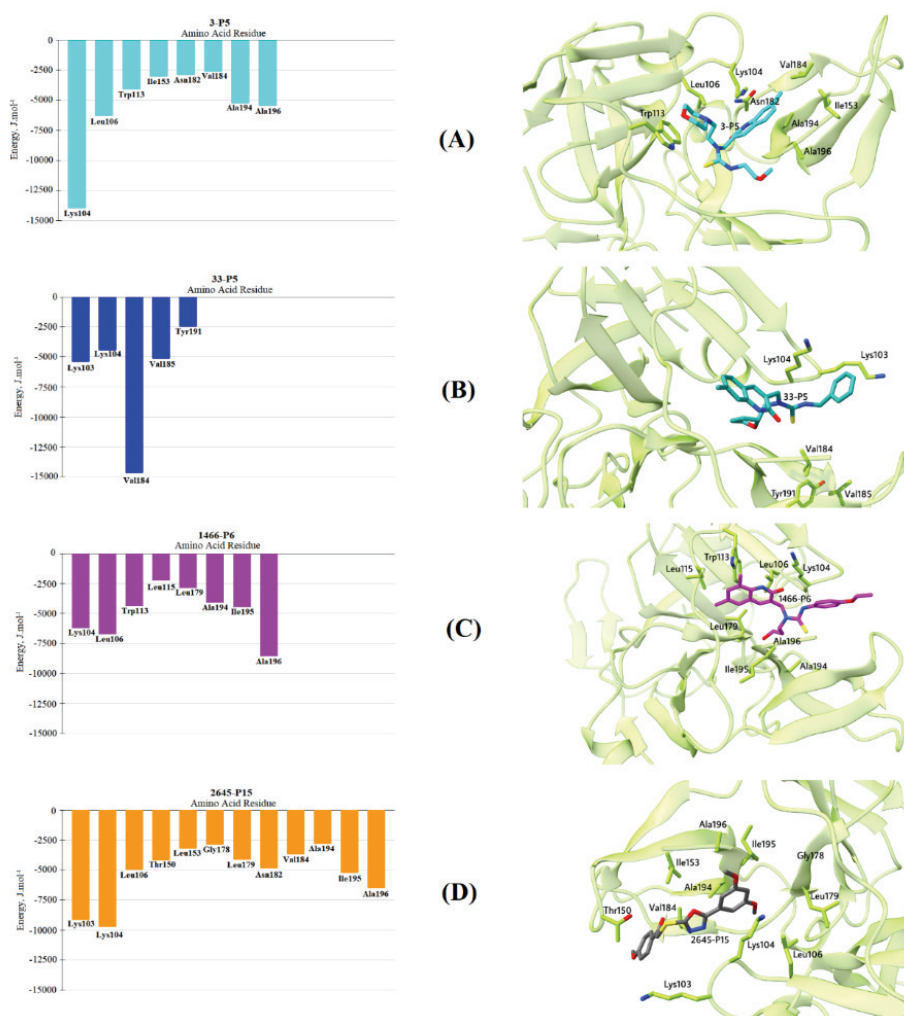


Fig. 2. Graphical representation of the interaction energy per residue (left) for the formed complexes: A) ligand 3-P5, B) ligand 33-P5, C) ligand 1466-P6 and D) ligand 2645-P15.

Analyzing the decomposition energy per residue of the NS2B/NS3pro structure complexed with ligand 2645-P15, it was observed that the residues Lys103 (73), Lys104 (74), Leu106 (76), Thr150 (120), Ile153 (123), Gly178 (148), Leu179 (149), Asn182 (152), Val184 (154), Ala194 (164), Ile195 (165) and Ala196 (166) from the NS2B/NS3pro allosteric site⁴³ formed favorable interactions with the aforementioned ligand, thus contributing to the stabilization of this complex. Of the other complex, 3-P5 presented the second lowest affinity energy and from an analysis of the residues that contribute favorably to the interaction with it, the influence of Lys104 (74), Leu106 (76), Trp113 (83), Ile153 (123), Asn182 (152), Val184 (154), Ala194 (164) and Ala196 (166). For the ligand 1466-P6, the residues Lys104 (74), Leu106 (76), Trp113 (83), Leu115 (85), Leu179 (149), Ala194 (164), Ile195 (165), Ala196 (166) were the main contributors to stability and to ligand 33-P5, the residues Lys103 (73), Lys104 (74), Val184 (154), Tyr191(161) and Val185(155) had favorable contributions. All ligands present favorable interactions that stabilized the complexes with residues from the NS2B/NS3pro allosteric site.^{7,19,43} Therefore, inhibitors targeting this pocket may potentially be broad spectrum flavivirus inhibitors.

The residues Lys104(74) and Leu106(76) contribute significantly to the four simulated complexes. However, the interaction of Lys104(74) with the double benzene ring of the 3-P5 ligand is 1 kcal* mol⁻¹ greater than that of the other systems, which is also well highlighted for the 2645-P15 ligand that also undergoes hydrogen bonding interaction with Thr150, is well highlighted. The triad of residues Ala194(164), Ile195(165), and Ala196(166) seems to contribute to the stabilization of the ligands at this site, especially in the systems of ligands 33-P5 and ligand 1466-P6. Based on this strong link with the triad, structural modifications to obtain more promising compounds are possible.

Although the two systems share similar bonds and interactions, which ensures that the inhibitors can bind tightly to the receptor protein, the existence of subtle discrepancies can be used in the future for designing drugs having these residues, with a high binding capacity.

The favorable interactions presented for the 3-P5 and 2645-P15 ligands corroborate the results observed in the literature that report NS2B/NS3pro allosteric inhibitors *in silico* and *in vitro* studies.^{38,43,45,46} This fact suggests that these ligands may show inhibitory activity directed at the NS2B/NS3pro allosteric site.

In particular, analyzing the ligand 2645-P15, which showed the best binding affinities (ΔG_{bind}) based on the MM/GBSA method, it was possible to observe interactions with the residue Lys103 (73), Lys104 (74), Leu179 (149) and Asn182 (152), Val184(154) that, according to experimental and theoretical studies, are essential for protease inhibition.^{19,38,43,45} Othman and collaborators⁴⁶ observed that interactions with residues Lys104 (74) and Leu179 (149) explained

* 1 kcal = 4184 J

the difference in the inhibition activity of non-competitive inhibitors in their studies. This interaction with Lys104 (74) is directly linked to Asp75 inducing a change in the region of the catalytic triad. This, presumably, could interrupt the electron transfer process necessary for the binding of the substrate at the active site, thus affecting the activity of the protease. Herein, the effects of the protein environment on the ligand binding could be highlighted. Some reports have considered the protonation pattern of the protein system determined by calculating the electrostatic energies from the solution of the linearized Poisson–Boltzmann Equation (LPBE).^{47,48} The present results using an empirical approach (H++ server) indicate that the protonation states are in accordance with other studies, as mentioned above. Finally, it should be stressed that Leu179 (149) residue plays a role in the inhibition activity by blocking the entry of the ligand into the active site due to its position in the protease.^{38,46}

CONCLUSIONS

In the present study, molecular docking, MD simulations and binding free energy calculations were used to investigate the binding affinity, selectivity and stability of candidates for allosteric inhibitors of the DENV NS2B/NS3pro enzyme. GOLD and DOCK6 programs were used to filter 3940 compounds through consensual docking, where the best positions were chosen based on the docking energies and hydrogen bonds. To estimate the dynamic behavior, MD simulations were performed for four protein–ligand complexes that proved to be promising in the consensual approach, and simulations of 100 ns each were performed using the AMBER package. The binding free energies were calculated for the simulated systems, highlighting the ligands 3-P5 and 2645-P15 that presented interactions with several residues of interest, these results are consistent with the results of other studies. Among them, the residues Lys103 (73), Asn182 (152), Lys104 (74) and Leu179 (149) are highlight. In addition, the triad of residues Ala194(164), Ile195(165), and Ala196(166) seems to be important in the stability of all systems and could be explored in the future when designing new compounds. The computational approach used herein proved to be useful for designing new inhibitors to combat Dengue.

SUPPLEMENTARY MATERIAL

Docking energy values for all compounds obtained by the GOLD and DOCK6 programs and their final classification values collected by the consensus platform Additional data and information are available electronically at the pages of journal website: <https://www.shd-pub.org.rs/index.php/JSCS/article/view/11230>, or from the corresponding author on request.

ИЗВОД

IN SILICO ИДЕНТИФИКАЦИЈА НОВИЈИХ АЛОСТЕРИЧНИХ ИНХИБИТОРА СЕРИН
ПРОТЕАЗЕ ДЕНГА ВИРУСА NS2B/NS3

RENATO A. DA COSTA¹, JOÃO A. P. DA ROCHA², ALAN S. PINHEIRO³, ANDRÉIA S. S. DA COSTA⁴, ELAINE C. M. DA ROCHA⁵, LUIZ P. C. JOSINO³, ARLAN DA SILVA GONÇALVES⁶, ANDERSON H. L. LIMA³ и DAVI S. B. BRASIL⁴

¹Federal Institute of Education, Science and Technology of Pará - Campus Castanhal, 68740-970, Castanhal-PA, Brazil, ²Federal Institute of Education, Science and Technology of Pará – Campus Bragança, 68600-000, Bragança-PA, Brazil, ³Graduate Program in Chemistry, Institute of Exact and Natural Sciences, Federal University of Pará (UFPA), 66075-110 Belém-PA, Brazil, ⁴Graduate Program in Science and Environment, Institute of Exact and Natural Sciences, Federal University of Pará (UFPA), 66075-110 Belém-PA, Brazil, ⁵Federal Rural University of the Amazon Campus Capanema (UFRA), 68700-665 Capanema-PA, Brazil u ⁶Federal Institute of Education, Science and Technology Technology of Espírito Santo Campus Vila Velha, 29106-010 Vila Velha-ES, Brazil

Иако је Денга грозница болест која напада преко 100 земаља и сваке године излаже опасности скоро 400 милиона живота, нема одобреног антивирусног лека за третирање ове патологије. У том контексту, протеазе су потенцијални биолошки циљеви пошто су оне битне у процесу умножавања овог вируса. У овој студији је коришћена библиотека са више од 3000 структура да би се истражила алостеричка инхибиција NS2B/NS3 комплекса протеаза коришћењем техника сагласног докинга (consensual docking techniques). Резултати показују четири најбоље рангиране структуре које су одабране за симулације молекулске динамике и слободне енергије. Наша анализа је подржана другим студијама (експерименталним и теоријским) изнесеним у литератури. Тако је показано да овде коришћен рачунарски приступ може бити користан за планирање нових инхибитора у борби против Денга болести.

(Примљено 29. септембра 2021, ревидирано 20. јануара, прихваћено 17. фебруара 2022)

REFERENCES

1. A. Wilder-Smith, Murray, M. Quam, *Clin. Epidemiol.* (2013) 299 (<https://doi.org/10.2147/CLEP.S34440>)
2. M. G. Guzman E. Harris, *Lancet* **385** (2015) 453 ([https://doi.org/10.1016/S0140-6736\(14\)60572-9](https://doi.org/10.1016/S0140-6736(14)60572-9))
3. S. Bhatt, P. W. Gething, O. J. Brady, J. P. Messina, A. W. Farlow, C. L. Moyes, J. M. Drake, J. S. Brownstein, A. G. Hoen, O. Sankoh, M. F. Myers, D. B. George, T. Jaenisch, G. R. W. Wint, C. P. Simmons, T. W. Scott, J. J. Farrar, S. I. Hay, *Nature* **496** (2013) 504 (<https://doi.org/10.1038/nature12060>)
4. C. P. Simmons, K. McPherson, N. Van Vinh Chau, D. T. Hoai Tam, P. Young, J. Mackenzie, B. Wills, *Vaccine* **33** (2015) 7061 (<https://doi.org/10.1016/j.vaccine.2015.09.103>)
5. K. V Pugachev, F. Guirakhoo, D. W. Trent, T. P. Monath, *Int. J. Parasitol.* **33** (2003) 567 ([https://doi.org/10.1016/S0020-7519\(03\)00063-8](https://doi.org/10.1016/S0020-7519(03)00063-8))
6. D. Luo, S. G. Vasudevan, J. Lescar, *Antiviral Res.* **118** (2015) 148 (<https://doi.org/10.1016/j.antiviral.2015.03.014>)
7. M. Yildiz, S. Ghosh, J. A. Bell, W. Sherman, J. A. Hardy, *ACS Chem. Biol.* **8** (2013) 2744 (<https://doi.org/10.1021/cb400612h>)
8. B. Millies, F. von Hammerstein, A. Gellert, S. Hammerschmidt, F. Barthels, U. Göppel, M. Immerheiser, F. Elgner, N. Jung, M. Basic, C. Kersten, W. Kiefer, J. Bodem, E. Hildt, M. Windbergs, U. A. Hellmich, T. Schirmeister, *J. Med. Chem.* **62** (2019) 11359 (<https://doi.org/10.1021/acs.jmedchem.9b01697>)

9. M. Merdanovic, T. Mönig, M. Ehrmann, M. Kaiser, *ACS Chem. Biol.* **8** (2013) 19 (<https://doi.org/10.1021/cb3005935>)
10. M. Aminpour, C. Montemagno, J. A. Tuszynski, *Molecules* **24** (2019) 1693 (<https://doi.org/10.3390/molecules24091693>)
11. T. Casalini, *J. Control. Rel.* **332** (2021) 390 (<https://doi.org/10.1016/j.jconrel.2021.03.005>)
12. B. S. Kolte, S. R. Londhe, B. R. Solanki, R. N. Gacche, R. J. Meshram, *J. Mol. Graph. Model.* **80** (2018) 95 (<https://doi.org/10.1016/j.jmgm.2017.12.020>)
13. P. Erbel, N. Schiering, A. D'Arcy, M. Rénatus, M. Kroemer, S. P. Lim, Z. Yin, T. H. Keller, S. G. Vasudevan, U. Hommel, *Nat. Struct. Mol. Biol.* **13** (2006) 372 (<https://doi.org/10.1038/nsmb1073>)
14. R. Perez-Pineiro, A. Burgos, D. C. Jones, L. C. Andrew, H. Rodriguez, M. Suarez, A. H. Fairlamb, D. S. Wishart, *J. Med. Chem.* **52** (2009) 1670 (<https://doi.org/10.1021/jm801306g>)
15. M. D. de Oliveira, J. de O. Araújo, J. M. P. Galúcio, K. Santana, A. H. Lima, *J. Mol. Graph. Model.* **101** (2020) 107735 (<https://doi.org/10.1016/j.jmgm.2020.107735>)
16. E. Harigua-Souiai, Y. Z. Abdelkrim, I. Bassoumi-Jamoussi, O. Zakraoui, G. Bouvier, K. Essafi-Benkhadir, J. Banroques, N. Desdouits, H. Munier-Lehmann, M. Barhoumi, N. K. Tanner, M. Nilges, A. Blondel, I. Guizani, *PLoS Negl. Trop. Dis.* **12** (2018) e0006160 (<https://doi.org/10.1371/journal.pntd.0006160>)
17. G. Jones, P. Willett, R. C. Glen, *J. Mol. Biol.* **245** (1995) 43 ([https://doi.org/10.1016/s0022-2836\(95\)80037-9](https://doi.org/10.1016/s0022-2836(95)80037-9))
18. S. R. Brozell, S. Mukherjee, T. E. Balias, D. R. Roe, D. A. Case, R. C. Rizzo, *J. Comput. Aided Mol. Des.* **26** (2012) 749 (<https://doi.org/10.1007/s10822-012-9565-y>)
19. M. Brecher, Z. Li, B. Liu, J. Zhang, C. A. Koetzner, A. Alifarag, S. A. Jones, Q. Lin, L. D. Kramer, H. Li, *PLoS Pathog.* **13** (2017) e1006411 (<https://doi.org/10.1371/journal.ppat.1006411>)
20. E. C. Meng, B. K. Shoichet, I. D. Kuntz, *J. Comput. Chem.* **13** (1992) 505 (<https://doi.org/10.1002/jcc.540130412>)
21. I. D. Kuntz, J. M. Blaney, S. J. Oatley, R. Langridge, T. E. Ferrin, *J. Mol. Biol.* **161** (1982) 269 ([https://doi.org/10.1016/0022-2836\(82\)90153-X](https://doi.org/10.1016/0022-2836(82)90153-X))
22. A. S. Pinheiro, J. B. C. Duarte, C. N. Alves, F. A. de Molfetta, *Appl. Biochem. Biotechnol.* **176** (2015) 1709 (<https://doi.org/10.1007/s12010-015-1672-5>)
23. J. M. Wang, R. M. Wolf, J. W. Caldwell, P. A. Kollman, D. A. Case, *J. Comput. Chem.* **25** (2004) 1157 (<https://doi.org/10.1002/jcc.20035>)
24. J. A. Maier, C. Martinez, K. Kasavajhala, L. Wickstrom, K. E. Hauser, C. Simmerling, *J. Chem. Theory Comput.* **11** (2015) 3696 (<https://doi.org/10.1021/acs.jctc.5b00255>)
25. P. A. Kollman, I. Massova, C. Reyes, B. Kuhn, S. Huo, L. Chong, M. Lee, T. Lee, Y. Duan, W. Wang, O. Donini, P. Cieplak, J. Srinivasan, D. A. Case, T. E. Cheatham, *Acc. Chem. Res.* **33** (2000) 889 (<https://doi.org/10.1021/ar000033j>)
26. *Gaussian 09 software*, Pittsburgh, PA, 2016
27. R. Anandakrishnan, B. Aguilar, A. V. Onufriev, *Nucleic Acids Res.* **40** (2012) W537 (<https://doi.org/10.1093/nar/gks375>)
28. W. L. Jorgensen, J. Chandrasekhar, J. D. Madura, R. W. Impey, M. L. Klein, *J. Chem. Phys.* **79** (1983) 926 (<https://doi.org/10.1063/1.445869>)
29. T. Darden, D. York, L. Pedersen, *J. Chem. Phys.* **98** (1993) 10089 (<https://doi.org/10.1063/1.464397>)
30. J. P. Ryckaert, G. Ciccotti, H. J. C. Berendsen, *J. Comput. Phys.* **23** (1977) 327 ([https://doi.org/10.1016/0021-9991\(77\)90098-5](https://doi.org/10.1016/0021-9991(77)90098-5))

31. E. Wang, H. Sun, J. Wang, Z. Wang, H. Liu, J. Z. H. Zhang, T. Hou, *Chem. Rev.* **119** (2019) 9478 (<https://doi.org/10.1021/acs.chemrev.9b00055>)
32. P. A. Kollman, I. Massova, C. Reyes, B. Kuhn, S. Huo, L. Chong, M. Lee, T. Lee, Y. Duan, W. Wang, O. Donini, P. Cieplak, J. Srinivasan, D. A. Case, T. E. Cheatham, *Acc. Chem. Res.* **33** (2000) 889 (<https://doi.org/10.1021/ar000033j>)
33. S. Genheden U. Ryde, *Expert Opin. Drug Discov.* **10** (2015) 449 (<https://doi.org/10.1517/17460441.2015.1032936>)
34. R. A. Costa, J. N. Cruz, F. C. A. Nascimento, S. G. Silva, S. O. Silva, M. C. Martelli, S. M. L. Carvalho, C. B. R. Santos, A. M. J. C. Neto, D. S. B. Brasil, *Med. Chem. Res.* **28** (2019) 246 (<https://doi.org/10.1007/s00044-018-2280-z>)
35. E. P. Semighini, J. A. Resende, P. de Andrade, P. A. B. Morais, I. Carvalho, C. A. Taft, C. H. T. P. Silva, *J. Biomol. Struct. Dyn.* **28** (2011) 787 (<https://doi.org/10.1080/07391102.2011.10508606>)
36. M. Hariono, S. B. Choi, R. F. Roslim, M. S. Nawi, M. L. Tan, E. E. Kamarulzaman, N. Mohamed, R. Yusof, S. Othman, N. Abd Rahman, R. Othman, H. A. Wahab, *PLOS One* **14** (2019) e0210869 (<https://doi.org/10.1371/journal.pone.0210869>)
37. A. J. Fathima, G. Murugaboopathi, P. Selvam, *Curr. Bioinform.* **13** (2018) 606 (<https://doi.org/10.2174/1574893613666180118105659>)
38. A. Mukhametov, E. I. Newhouse, N. A. Aziz, J. A. Saito, M. Alam, *J. Mol. Graph. Model.* **52** (2014) 103 (<https://doi.org/10.1016/j.jmgm.2014.06.008>)
39. F. A. D. M. Opo, M. M. Rahman, F. Ahammad, I. Ahmed, M. A. Bhuiyan, A. M. Asiri, *Sci. Rep.* **11** (2021) 4049 (<https://doi.org/10.1038/s41598-021-83626-x>)
40. A. Fornili, F. Autore, N. Chakroun, P. Martinez, F. Fraternali, *Computational Drug Discovery and Design*, Springer, New York, 2011, p. 375 (https://doi.org/10.1007/978-1-61779-465-0_23)
41. M. Shahbaaz, A. Nkaule, A. Christoffels, *Sci. Rep.* **9** (2019) 4405 (<https://doi.org/10.1038/s41598-019-40621-7>)
42. F. Ghasemi, A. Zomorodipour, A. A. Karkhane, M. R. Khorramzadeh, *J. Mol. Graph. Model.* **68** (2016) 39 (<https://doi.org/10.1016/j.jmgm.2016.05.011>)
43. H. Wu, S. Bock, M. Snitko, T. Berger, T. Weidner, S. Holloway, M. Kanitz, W. E. Diederich, H. Steuber, C. Walter, D. Hofmann, B. Weißbrich, R. Spannaus, E. G. Acosta, R. Bartenschlager, B. Engels, T. Schirmeister, J. Bodem, *Antimicrob. Agents Chemother.* **59** (2015) 1100 (<https://doi.org/10.1128/AAC.03543-14>)
44. R. A. Costa, J. N. Cruz, F. C. A. Nascimento, S. G. Silva, S. O. Silva, M. C. Martelli, S. M. L. Carvalho, C. B. R. Santos, A. M. J. C. Neto, D. S. B. Brasil, *Med. Chem. Res.* **28** (2019) 246 (<https://doi.org/10.1007/s00044-018-2280-z>)
45. B. Millies, F. von Hammerstein, A. Gellert, S. Hammerschmidt, F. Barthels, U. Göppel, M. Immerheiser, F. Elgner, N. Jung, M. Basic, C. Kersten, W. Kiefer, J. Bodem, E. Hildt, M. Windbergs, U. A. Hellmich, T. Schirmeister, *J. Med. Chem.* **62** (2019) 11359 (<https://doi.org/10.1021/acs.jmedchem.9b01697>)
46. R. Othman, T. S. Kiat, N. Khalid, R. Yusof, E. Irene Newhouse, J. S. Newhouse, M. Alam, N. A. Rahman, *J. Chem. Inf. Model.* **48** (2008) 1582 (<https://doi.org/10.1021/ci700388k>)
47. D. Popovic I. Djordjevic, *J. Serb. Chem. Soc.* **85** (2020) 1429 (<https://doi.org/10.2298/JSC200720047P>)
48. D. M. Popović A. A. Stuchebrukhov, *J. Am. Chem. Soc.* **126** (2004) 1858 (<https://doi.org/10.1021/ja038267w>).